



Performance Evaluation of a Single-Phase Grid-Forming Inverter Through Hardware Experiments

Preprint

Jing Wang, Subhankar Ganguly, Soham Chakraborty, and Benjamin Kroposki

National Renewable Energy Laboratory

*Presented at the 2024 IEEE Energy Conversion Congress & Expo (ECCE)
Phoenix, Arizona
October 20–24, 2024*

**NREL is a national laboratory of the U.S. Department of Energy
Office of Energy Efficiency & Renewable Energy
Operated by the Alliance for Sustainable Energy, LLC**

This report is available at no cost from the National Renewable Energy Laboratory (NREL) at www.nrel.gov/publications.

Contract No. DE-AC36-08GO28308

Conference Paper
NREL/CP-5D00-89026
October 2024



Performance Evaluation of a Single-Phase Grid-Forming Inverter Through Hardware Experiments

Preprint

Jing Wang, Subhankar Ganguly, Soham Chakraborty, and Benjamin Kroposki

National Renewable Energy Laboratory

Suggested Citation

Wang, Jing, Subhankar Ganguly, Soham Chakraborty, and Benjamin Kroposki. 2024. *Performance Evaluation of a Single-Phase Grid-Forming Inverter Through Hardware Experiments: Preprint*. Golden, CO: National Renewable Energy Laboratory. NREL/CP-5D00-89026. <https://www.nrel.gov/docs/fy25osti/89026.pdf>.

© 2024 IEEE. Personal use of this material is permitted. Permission from IEEE must be obtained for all other uses, in any current or future media, including reprinting/republishing this material for advertising or promotional purposes, creating new collective works, for resale or redistribution to servers or lists, or reuse of any copyrighted component of this work in other works.

**NREL is a national laboratory of the U.S. Department of Energy
Office of Energy Efficiency & Renewable Energy
Operated by the Alliance for Sustainable Energy, LLC**

This report is available at no cost from the National Renewable Energy Laboratory (NREL) at www.nrel.gov/publications.

Contract No. DE-AC36-08GO28308

Conference Paper
NREL/CP-5D00-89026
October 2024

National Renewable Energy Laboratory
15013 Denver West Parkway
Golden, CO 80401
303-275-3000 • www.nrel.gov

NOTICE

This work was authored by the National Renewable Energy Laboratory, operated by Alliance for Sustainable Energy, LLC, for the U.S. Department of Energy (DOE) under Contract No. DE-AC36-08GO28308. This material is based upon work supported by the U.S. Department of Energy's Office of Energy Efficiency and Renewable Energy (EERE) under Solar Energy Technologies Office (SETO) Agreement Number 38637. The views expressed herein do not necessarily represent the views of the DOE or the U.S. Government.

This report is available at no cost from the National Renewable Energy Laboratory (NREL) at www.nrel.gov/publications.

U.S. Department of Energy (DOE) reports produced after 1991 and a growing number of pre-1991 documents are available free via www.OSTI.gov.

Cover Photos by Dennis Schroeder: (clockwise, left to right) NREL 51934, NREL 45897, NREL 42160, NREL 45891, NREL 48097, NREL 46526.

NREL prints on paper that contains recycled content.

Performance Evaluation of a Single-Phase Grid-Forming Inverter Through Hardware Experiments

Jing Wang, Subhankar Ganguly, Soham Chakraborty, Benjamin Kroposki

Power Systems Engineering Center, National Renewable Energy Laboratory, Golden, Colorado 80401, USA.

{jing.wang, subhankar.ganguly, soham.chakraborty, benjamin.kroposki}@nrel.gov

Abstract—This study conducts hardware experiments to assess the performance of a commercial single-phase grid-forming (GFM) inverter using a purely hardware-based approach. We adhere to a testing protocol for the GFM inverter and enhance it by exploring the transient performance of GFM inverters across various grid dynamic events. Quantifiable performance metrics are established for each testing scenario to gain insights into the performance of the single-phase GFM inverters. Based on the comprehensive tests, the following observations are summarized: 1) The performance of the single-phase GFM inverter is satisfactory, and it is capable of being the islanding master for residence homes when the main grid is gone. 2) For frequency response, the inverter is able to stay connected but cannot inject the needed active power to support the grid. This may be improved by the manufacturer by using droop control. 3) The GFM inverter exhibits harmful transients in voltage and frequency during islanding operation, which can be enhanced by maintaining the same operating points before and after the breaker is open.

Index Terms—Black start, droop control, grid-forming inverters, grid-following inverters, transient stability.

I. INTRODUCTION

Grid-forming (GFM) inverters are recognized as enabling technologies for integrating inverter-based resources (IBRs) into electric grids, across microgrids, and in distribution and transmission networks [1]. In particular, GFM inverters have been widely used in microgrid applications as the GFM source(s) to enhance system resilience [2]. GFM inverters are also used for large island systems—such as AEMO, ENTSO-E, HECO, KIUC, and Fingrid—to increase system strength in weak grid areas and to enable the integration of more renewable [3]. But those are three-phase inverters, and the ever-increasing integration of distributed energy resources (DERs) in distribution systems necessitates similar solutions for single-phase inverters [4]. A comprehensive literature review shows that the research activities on single-phase GFM inverters have

This work was supported by Alliance for Sustainable Energy, LLC, the manager and operator of the National Renewable Energy Laboratory for the U.S. Department of Energy (DOE) under Contract No. DE-AC36-08GO28308. This material is based upon work supported by the U.S. Department of Energy’s Office of Energy Efficiency and Renewable Energy (EERE) under Solar Energy Technologies Office (SETO) Agreement Number 38637. The views expressed in the article do not necessarily represent the views of the DOE or the U.S. Government. The U.S. Government retains and the publisher, by accepting the article for publication, acknowledges that the U.S. Government retains a nonexclusive, paid-up, irrevocable, worldwide license to publish or reproduce the published form of this work, or allow others to do so, for U.S. Government purposes.

primarily focused on transient stability analysis [5], black-start reconnection procedures [6], control strategies [7], [8], harmonic compensation [9], and large-signal stability analysis [10].

The existing state of the art explores single-phase GFM inverters from different aspects through electromagnetic transient simulations; however, very few works perform hardware tests, and there is no clear understanding of how single-phase GFM inverters should behave from a hardware perspective. Therefore, this paper addresses these gaps by performing hardware experiments to evaluate the performance of a single-phase GFM hardware inverter. The main contributions of the paper are to: (1) enrich the standard testing protocols (e.g., characterization approaches and scenarios) with a comprehensive performance evaluation of single-phase GFM inverters; (2) provide insights on the performance and functionality of single-phase GFM inverters; and (3) suggest performance improvements for the tested single-phase GFM inverters.

II. THE CHARACTERIZATION TEST

A. Testing Objective and Scenarios

The objective of the performance evaluation is to comprehensively evaluate single-phase GFM inverters under a wide range of operating conditions, including stand-alone (microgrid), grid-connected, and transition operations. In particular, we investigate the steady-state and transient performance of the inverter’s (1) PQ capability, dispatchability, overloading capability, step response, black-start capability, and smooth transition operation capability; and (2) dynamic response under grid events, output impedance characteristics and damping ratio, and inertia response. We follow the testing protocol from [11] and enrich it by adding the dynamic test scenarios marked in blue in Table 1, which summarizes the test scenarios and the corresponding quantifiable performance metrics. The variables are defined as follows: V_{rms} and I_{rms} (voltage and current root mean square), f (frequency), P and Q (active and reactive power), V_{inst} and I_{inst} (voltage and current instantaneous values), THD (total harmonic distortion), ΔP (active power output), f_0 (pre-fault system frequency), and S_{rating} (inverter rating).

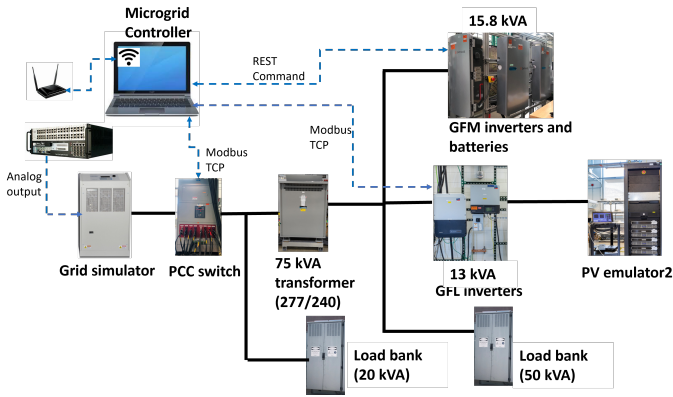


Fig. 1: Laboratory experiment setup.

B. Description of the GFM Inverter

The GFM inverter under test is an off-the-shelf inverter with a capacity of 3.8 kVA, and four inverters are operated in parallel for a total capacity of 15.2 kVA. The inverters always operate in GFM control even if they are grid-connected. Based on the manual, the inverters operate in isochronous mode without droop, and an automated secondary control will be issued to regulate the system voltage and frequency back to the nominal values after every dynamic event.

C. The Test Circuit

Fig. 1 shows the test circuit, which includes four GFM inverters with a battery on the DC side for each inverter, a point of common coupling (PCC) breaker, the GFL inverter DER rack (13 kVA, including two PV inverters and one battery inverter), two load banks, a 75-kVA single-phase transformer, and a grid simulator (45 kVA). This is the full circuit, and only a subset of devices will be used for any given test scenario. A microgrid controller is used to communicate with the GFM inverters via REST command, and the GFL inverters and the PCC switch via Modbus TCP/IP. OPAL-RT is used to drive the grid simulator with dynamic changes in the grid voltage through analog output.

III. EXPERIMENTAL RESULTS

The experimental tests are performed based on the test scenarios defined in Table 1. Due to the limited space of the paper, only the critical testing results are presented here.

A. Black Start

For this black start test, the load is PF 0.8 lagging. The test circuit is shown in Fig. 1 which includes the 277 V and 240 V circuits. The black start testing procedures are described as follows: (1) Start the GFM inverters and energize the 75-kVA 240/277 transformer; (2) bring in a 10-kVA load at the 480-V side; (3) bring in the GFL inverter with 5 kVA and dispatch full power; (4) bring in the second GFL inverter (3.8 kVA) and dispatch full power; (5) bring in the 6-kVA load at the 240-V side; and (6) bring in another 6 kVA at the 240-V side. The results presented in Fig. 2 show that the

black start is successful. The first spike is from energizing the transformer, which brings the GFM inverter voltage down to 0.87 p.u. with a 1.35-p.u. inrush current and a 60.6-Hz frequency peak. During the black-start process of connecting the loads and GFL inverters, the GFM inverters show smooth transients. Note that the GFM inverters always try to settle to their nominal voltage and frequency after every step within 10 s. The voltage and current THD are maintained below 2% and 5%, respectively.

B. Sourcing and Sinking Active Power

For the sourcing (generating) and sinking (absorbing) active power test, the test circuit includes the GFM inverter, the single-phase load (240 V), the PCC switch, and the grid simulator (240 V). In this grid-connected mode, the GFM inverter is dispatched to output the target active power. Note that this single-phase GFM inverter is not configured to support reactive power as we didn't have voltage related commands, hence the reactive power dispatch function cannot be tested. The target active power is to generate 25%, 50%, 75%, and 100% active power for the first test, and the second test is to absorb 25%, 50%, 75%, and 100% active power. The testing results are shown in Fig. 3 and Fig. 4.

The results show that the GFM inverter can follow the dispatched active power setpoint to output the target power. The average responding time is 0.1 s. There are some small amount of reactive power generated when only the active power is dispatched. The inverter's frequency is maintained around 60 Hz, and the inverter's voltage shows some jitters and keeps increasing/decreasing in one direction. For sourcing power, the voltage THD is below 1% and the current THD is below 6% for 25% power and below 3% for 50% and higher power. For sinking power, the voltage THD is below 2% and increasing with active power; and the current THD is 6% for 25% power and below 5% for 50% and higher power. The THD in sinking power mode is higher than sourcing power mode. This test shows the GFM inverter can be dispatched like a GFL inverter to output the target power in the grid-connected mode.

C. Dynamic Events

The testing circuit is the same as the sourcing and sinking active power test. The test results are summarized in Table. IV, which shows that the GFM inverters pass most of the dynamic event tests except the last two phase jumps. Overall, the results indicate that the GFM inverters are robust to system transients. To understand the behavior of the GFM inverters under the dynamic events, the results of the voltage down, frequency down, and phase jump up are presented in Fig. 5. For the voltage down, the inverter response time is 0.01 s, and the setting time is 0.47 s; for the frequency down, the inverter's response time is 0.02 s, and the setting time is 0.32 s; and for the phase jump up, the inverter's response time is 0.01 s, and the settling time is less than 1.3 s. Zoomed-in plots of voltage down shows that the reactive power is positive when the grid voltage is down, which is as expected. However, the

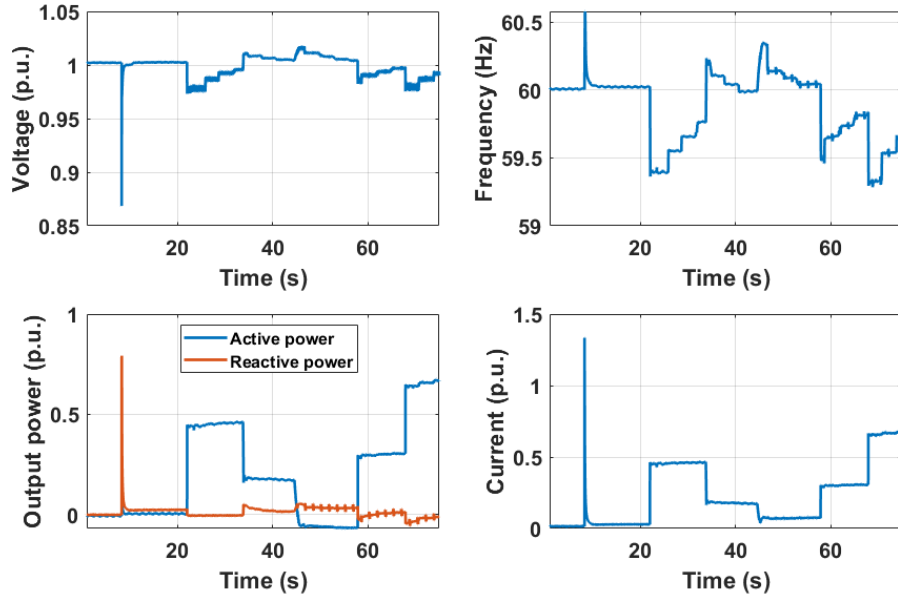


Fig. 2: Test results of black start with PF 0.8 lagging load.

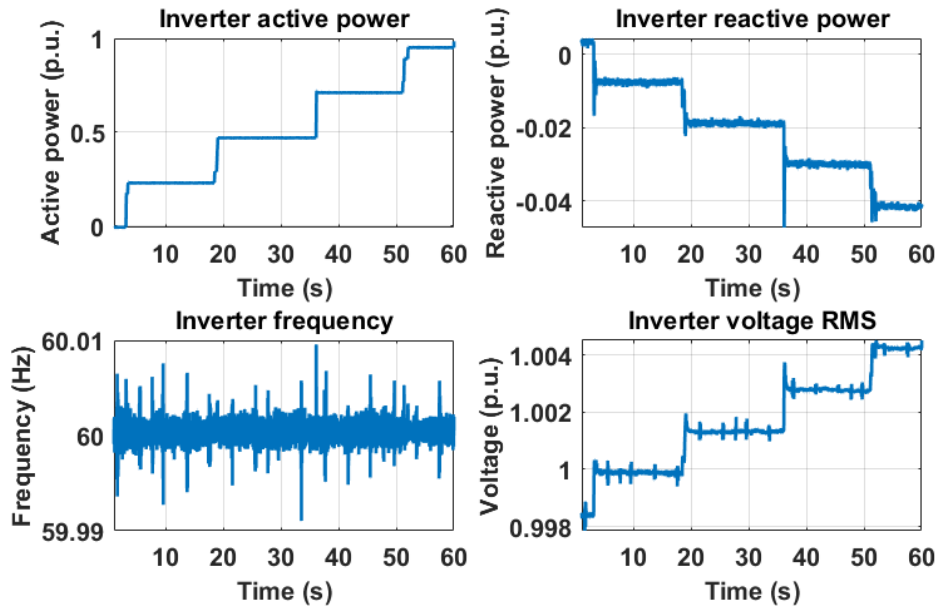


Fig. 3: The GFM inverter sourcing active power.

frequency jumping down caused a negative active power. The phase up caused an increase in the frequency, and a negative active power is observed, which is as expected. The responses of the GFM inverters under voltage and phase jump are as expected, and the response for frequency jump needs to be improved.

D. ROCOF Test

For the ROCOF test, the test circuit is the same as the dynamic test. This test is to understand the GFM inverter's capability to respond to frequency changes by proving needed

active power. The test result is shown in Fig. 6. We can see from the results that the inverter does not trip and does not respond to the frequency changes. This can be understood from the fact that this GFM inverter always operates in isochronous mode. Thus, there is no droop-type of behavior that normal GFM inverters would have to respond to frequency changes.

E. Impedance Scan

This test circuit is the same as the dynamic event test. This test is conducted when the single-phase GFM IBR is perturbed by the positive-sequence components in the voltage waveform,

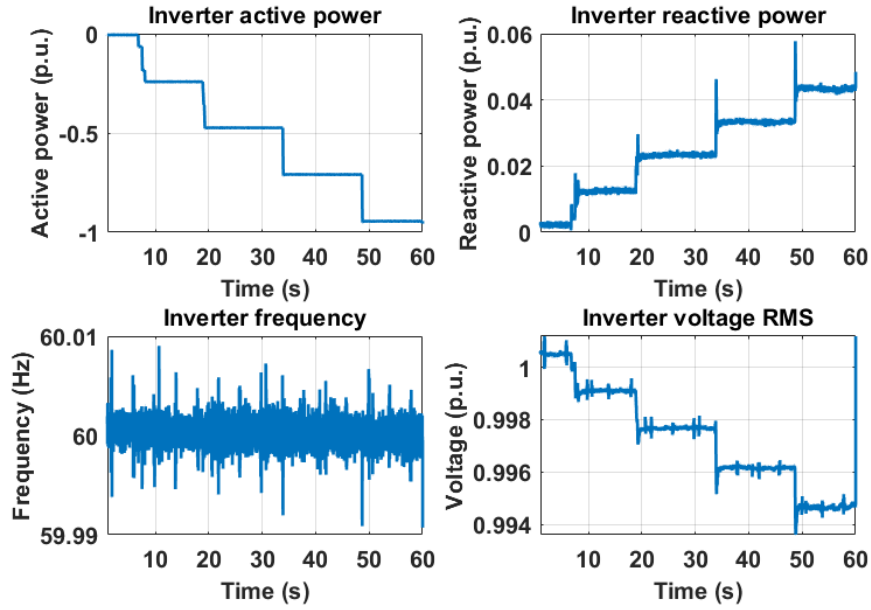


Fig. 4: The GFM inverter sinking active power.

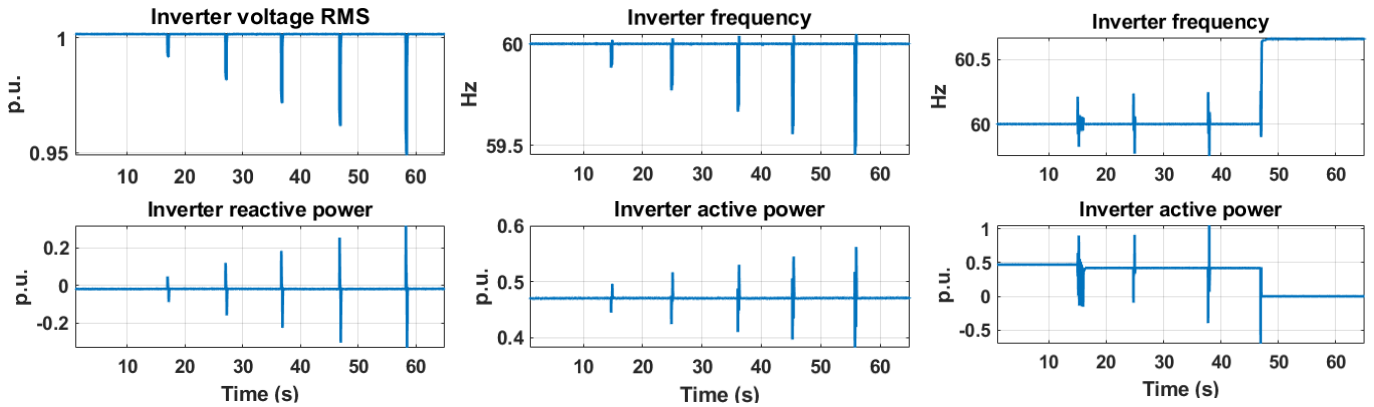


Fig. 5: Selected test results of dynamic events: voltage down (left), frequency down (middle), and phase jump up (right).

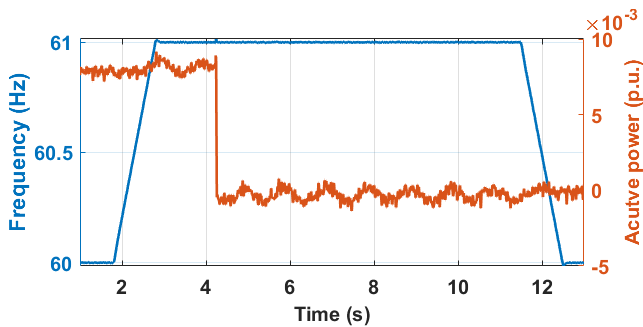


Fig. 6: The test results of ROCOF.

and the voltage and current measurements are collected to compute the output impedance $Z(s) = V(s)/(I(s))$. Note that perturbation harmonics are summarized in Table. I. The processed positive-sequence impedance, $|Z_P|$ (in dB), of the

single-phase GFM IBR, is shown in Fig. 7. Similarly, the measured phase of the positive-sequence impedance, $\angle Z_P$ (in deg), is shown in Fig. 7. In these figures, the blue circled data are the values computed based on the GFM IBR measurements. Based on the measured data of the magnitude, $|Z_P|$, and phase, $\angle Z_P$ (in deg), of the positive-sequence impedances, the best-fit transfer functions are estimated using the “tfest” command of the “System Identification Toolbox” of MATLAB. In the same figure, the Bode plots of the estimated transfer functions (piecewise) are also shown in red. This GFM inverter shows inductive characteristics at 60 Hz, and it is not damped at sub-synchronous frequency range. The closest non-piecewise transfer functions of the GFM inverter are shown in Table. III.

Note that the transfer functions are non-piecewise estimated transfer functions, which represent the piecewise transfer functions of Fig. 7, only inside the frequency range around the

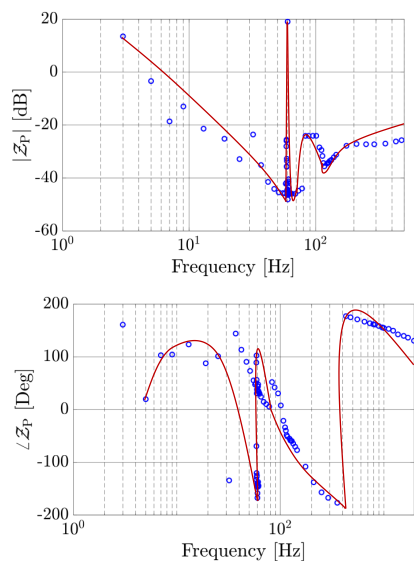


Fig. 7: The test results of impedance scan of the GFM inverter.

fundamental frequency as used in the piecewise transfer function computation. Based on the estimated and best-fit transfer function for each measured positive-sequence impedance, the equivalent damping coefficient, $\zeta_{\text{est}}^{\text{dut}}$, for the GFM inverter can be computed. The equivalent damping coefficient, $\zeta_{\text{est}}^{\text{dut}}$, for the single-phase GFM inverter is 0.33 ($2\zeta_{\text{est}}^{\text{dut}}\omega_R \approx 249.9.3$). This damping coefficient is aligned with the observation from Fig. 7.

F. Transition Operation

This test is completed with only the GFM inverter, the load, the PCC switch and the grid simulator. The test starts with islanded operation mode, then the small system (the GFM inverter and the load) synchronizes to the grid simulator. After working in grid-connected mode, the PCC circuit breaker is opened to allow for the islanding operation. Note that the GFM inverter is dispatched to supply the demand from the load when the PCC breaker is closed so that smooth transition operation can be achieved following the smooth transition operation protocol developed from the UNIFI 1MW demo test [11]. The results for synchronization and islanding operation are presented in Fig. 8 and Fig. 9.

Fig. 8 shows that the GFM inverter achieves smooth synchronization operation thanks to minimizing the PCC power flow (seen from the PCC current) before and after the breaker is closed and the GFM inverter maintains the same operating point during synchronization operation (seen from the inverter frequency, active power and current). For the islanding operation, the voltage of the GFM inverter shows some decaying oscillations for approximately 0.8 s and then reaches steady state, and the frequency has a sharp drop from 60 Hz to 58.5 Hz within 0.2 s. This islanding operation test is repeated a few times and consistent behaviors are observed.

IV. DISCUSSION

The testing scenarios summarized in Table. I are performed, and the testing results are summarized in Table. IV. This single-phase GFM inverter passed most of the tests, however, the dynamic events and ROCOF test are not as expected.

CONCLUSION

There is a lack of understanding of how hardware single-phase GFM inverters behave, especially under dynamic situations. This paper presents the comprehensive laboratory experimental testing of four hardware single-phase GFM inverters to understand their performance and functionalities. Following and enriching the testing protocol from [11], the performance and functionality of the single-phase GFM inverters is evaluated based on a variety of scenarios and performance metrics (e.g., power quality, overload capability, transient stability, and damping ratio). Overall, the performance of the single-phase GFM inverter is satisfactory and it is capable of being the islanding master for homes when the main grid is gone. Thus, this single-phase GFM inverter can be used as a GFM source to support the off-grid system for system resiliency. For frequency response, the inverter is able to stay connected but cannot inject the needed active power to support the grid. This may be improved by the manufacturer by using droop control. The islanding operation performance can be enhanced by maintaining the same operating points before and after the breaker is open. The performance of this GFM inverter can serve as a basis for single-phase inverters.

REFERENCES

- [1] M. Liu, W. Cai, S. Dhople, and B. Johnson, "Large-signal stability of phase-balanced equilibria in single-phase grid-forming inverter systems," *IEEE Tran. Power. Electron.*, vol. 39, no. 3, pp. 3623–3636, 2024.
- [2] J. Wang, C. Zhao, A. Pratt, and M. Baggu, "Design of an advanced energy management system for microgrid control using a state machine," *Applied Energy*, vol. 228, pp. 2407–2421, 2019.
- [3] "White paper: Grid forming functional specifications for bps-connected battery energy storage systems," tech. rep., 2023.
- [4] V. K. Nojima *et al.*, "A comparative analysis of voltage control methods for single-phase grid-forming inverters," in *2023 IEEE 2nd Industrial Electronics Society Annual On-Line Conference (ONCON)*, pp. 1–6, IEEE, 2023.
- [5] H. Rezazadeh, M. Monfared, M. Fazeli, and S. Golestan, "Single-phase grid-forming inverters: A review," in *2023 International Conference on Computing, Electronics Communications Engineering (iCCECE)*, pp. 1–6, IEEE, 2023.
- [6] G. Seo, J. Sawant, and F. Ding, "Black start of unbalanced microgrids harmonizing single- and three-phase grid-forming inverters," in *2023 IEEE Power Energy Society General Meeting (PESGM)*, pp. 1–6, IEEE, 2023.
- [7] A. Zarate, J. C. U. Pena, and D. S. Rosas, "Isolated and bidirectional two-state dc/ac converter with grid-forming virtual inertia and high ripple on the dc bus for single-phase grid application," in *2021 IEEE 12th International Symposium on Power Electronics for Distributed Generation Systems (PEDG)*, pp. 1–6, IEEE, 2021.
- [8] M. Momeni, L. Chang, and C. Diduch, "Modified andronov-hopf oscillator voltage control for single-phase grid forming inverters," in *2023 IEEE 14th International Conference on Power Electronics and Drive Systems (PEDS)*, pp. 1–6, IEEE, 2023.
- [9] S. Chen, Z. Chen, and W. Yu, "Multiple pr current regulator based dead-time effects compensation for grid-forming single-phase inverter," in *2018 IEEE Energy Conversion Congress and Exposition (ECCE)*, pp. 1–6, IEEE, 2018.

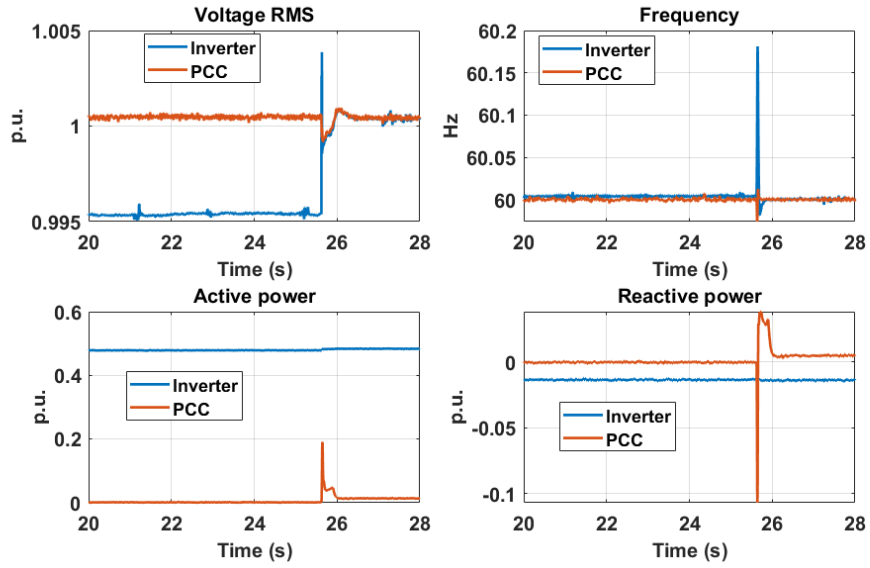


Fig. 8: Synchronization test results.

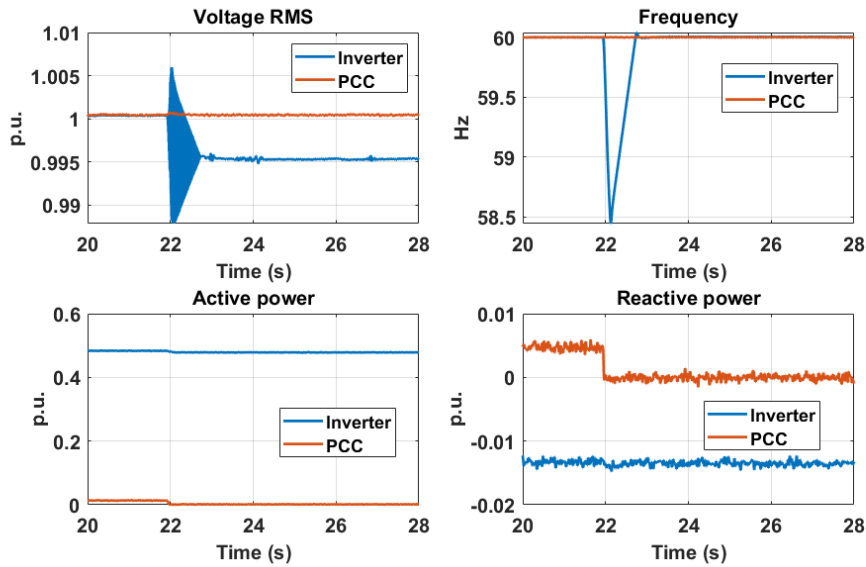


Fig. 9: Islanding operation test results.

[10] U. C. Nwaneto and A. M. Knight, "Using dynamic phasors to model and analyze selective harmonic compensated single-phase grid-forming inverter connected to nonlinear and resistive loads," *IEEE Tran. Ind. Electron.*, vol. 59, no. 5, pp. 6136–6154, 2023.

[11] J. Wang *et al.*, "Experimental characterization test of a grid-forming inverter for microgrid applications," in *2023 IEEE Energy Conversion Congress and Exposition (ECCE)*, pp. 1–6, IEEE, 2023.

TABLE I: Summary of all testing cases for individual inverter [11]

Configuration	Test Type	Scenario	Test Approach and Performance Metrics
Stand-alone operation	Steady state	Balanced load	Power factor (PF) 1, PF 0.8 lagging and leading, representing 5%, 10%, 25%, 50%, 75%, and 100% loading of the inverter capacity. Performance metrics: V_{rms} and f regulation; V_{rms} , I_{rms} , and THD of voltage and current
		Sinking power	The inverter will operate in parallel with a grid-following (GFL) inverter that is supplying more power than available load on the islanded power system. Performance metrics: V_{rms} and f regulation; V_{rms} , I_{rms} , and THD of voltage and current
	Transient	Black start	Starting from OFF, the inverter must energize a transformer of similar kVA size and connect the load(s) and GFL inverter(s) based on the predefined sequence. Performance metrics: V_{inst} and I_{inst} peak; V_{rms} and I_{rms} peak; V_{rms} and f settling time
		Load steps	Balanced linear load steps with PF of 1, 0.8 lagging, and 0.8 leading. The load steps will be performed from 0% to 50%, 50% to 100%, and 0% to 100% of the inverter kVA rating. Performance metrics: V_{inst} and I_{inst} peak; V_{inst} , I_{rms} , and f peak, nadir and settling time; V_{inst} transient distortion last more than 2–3 cycles
		Overload	The inverter will be subjected to 150% overcurrent at power factors of 1 and 0.8 lagging and leading. The overload will be held for x seconds and then indefinitely until the inverter trips. Performance metrics: Event duration: V_{rms} and f regulation; V_{rms} and I_{rms} , THD ; tripping time
		Loss of generator	The GFL inverter(s) is intentionally tripped off so that the GFM inverter will take over all the load and survive the islanded system. Performance metrics: V_{inst} and I_{inst} peak; V_{rms} , I_{rms} , and f peak, nadir and settling time; V_{inst} transient distortion
Grid-connected	Steady state	Sourcing and sinking active power	With the grid simulator set to the nominal voltage and frequency and the inverter voltage droop curve intercept set to achieve 0 or minimal reactive power flow, the inverter frequency droop curve intercept will be adjusted to force the inverter to source 5%, 10%, 25%, 50%, 75%, and 100% rated kW. With the inverter frequency droop curve intercept set to achieve 0 or minimal real power flow, the voltage droop curve intercept will be adjusted to force the inverter to source and sink 5%, 10%, 25%, 50%, 75%, and 100% rated kVAR. Performance metrics: V_{rms} , f , P , and Q regulation; V_{rms} and I_{rms} , THD ; oscillations
		Impedance scan	No load is connected. The GFM is dispatched with injecting 50% active power. The harmonic voltage perturbation is 1% of the fundamental component. The frequency sweep ranges from 3, 5, 7, 9, 13, 19, 25, 32, 37, 42, 47, 51, 55, 57, 58, 58.5, 58.6, 58.7, 58.8, 58.9, 59, 59.1, 59.2, 59.3, 59.4, 59.5, 59.7, 59.8, 59.9, 60.1, 60.2, 60.3, 60.5, 60.6, 60.7, 60.8, 60.9, 61, 61.1, 61.2, 61.3, 61.4, 61.5, 62, 63, 65, 69, 73, 78, 83, 88, 95, 101, 107, 111, 113, 115, 117, 123, 125, 127, 129, 133, 139, 145, 175, 210, 250, 290, 355, 430, 477, 554, 650, 733, 791, 821, 893, 965, 1000, 1113, 1231, 1370, 1557, 1712, 1957 Hz. Performance metrics: Output impedance (magnitude $ Z_P $ and phase angle $\angle Z_P$) and the equivalent damping ratio (ζ_{est}^{dut}) from a second-order system
	Transient	Dynamic event	PF1 load with 50% capacity of the GFM inverter, and the GFM inverter is dispatched by injecting 50% power. The grid simulator voltage magnitude, or frequency, or phase angle will be dynamically changed for 0.2 s and changed back. The voltage jumps up/down by 0.01, 0.02, 0.03, 0.04, and 0.05 p.u.; the frequency jumps up/down by 0.1, 0.2, 0.3, 0.4, and 0.5 Hz; and the phase jumps up/down by 5°, 10°, 15°, 20°, and 30°. Performance metrics: V_{inst} and I_{inst} peak; V_{rms} , I_{rms} , P , Q , and f peak, settling time; V_{inst} transient distortion; P and Q response time and settling time
		Inertia response test	PF=1 load with 50% capacity of the GFM inverter, and the GFM inverter is dispatched by injecting 0% power. The grid frequency will be changed with a rate of change of frequency (ROCOF) of 1 Hz/s at zero power or light loading (e.g., 20%). Performance metrics: equivalent inertia constant $H = (\Delta P * f_0) / (2S_{rating} * 1Hz/s)$
Transition operation	Transient	Synchronize a small system to the grid, and islanding	The inverter is initially operating as a single source energizing a local area power system. The local area power system can connect to a larger grid, which could be an actual utility grid or could be emulated using a grid simulator. Once the system is in steady state, planned islanding is performed. Performance metrics: V_{inst} and I_{inst} peak; V_{rms} , I_{rms} , P , Q , and f peak, nadir and settling time; V_{inst} transient distortion; time from when sync command issued until breaker closes.

TABLE II: Summary of dynamic event testing results.

Voltage jump (p.u.)	0.01	0.02	0.03	0.04	0.05	-0.01	-0.02	-0.03	-0.04	-0.05
Pass/Fail	✓	✓	✓	✓	✓	✓	✓	✓	✓	✓
Frequency jump (Hz)	0.1	0.2	0.3	0.4	0.5	-0.1	-0.2	-0.3	-0.4	-0.5
Pass/Fail	✓	✓	✓	✓	✓	✓	✓	✓	✓	✓
Phase jump (°)	5°	10°	15°	20°	30°	-5°	-10°	-15°	-20°	-30°
Pass/Fail	✓	✓	✓	×	×	✓	✓	✓	×	×

TABLE III: Non Piece-wise Transfer Functions of the GFM inverter and Equivalent Damping Coefficients.

DuT	Non-piece-wise Transfer Function	FitPercent	DuT	Damping
GFM-1	$\frac{0.712(s + 1.6 \times 10^4)(s + 3521)(s - 250)(s - 134.8)(s^2 + 3.29s + 1.525 \times 10^8)}{(s^2 + 249.9s + 1.432 \times 10^5)(s^2 + 870.7s + 1.32 \times 10^8)(s^2 + 3.59s + 1.5 \times 10^8)}$	96.87%	GFM-1	$\zeta_{est}^{dut} \approx 0.33$

TABLE IV: Summary of testing results

Configuration	Test Type	Scenario	Pass/Fail	Remark	
Stand-alone operation	Steady state	Balanced load	Pass	Whenever voltage decreases because of increasing load, the voltage tends to regulate slowly to its nominal values. The same happens to the frequency.	
		Sinking power	Pass	Follow the change of GFL inverter output well to adjust its active and reactive power output.	
	Transient	Black start	Pass	Fast black start capability.	
		Load steps	Pass	Can handle from 0% to 100% load step smoothly.	
		Overload	Pass	1.5 p.u. can last more than 10 s.	
Grid-connected	Steady state	Sourcing and sinking active power	Pass	Sinking power has higher voltage and current THD in sourcing power.	
		Impedance scan	Pass	Has similar output impedance characteristic and damping coefficient compared to the three-phase GFM inverters.	
	Transient	Dynamic event (voltage jump)	Pass	The GFM inverter does respond correctly to voltage changes.	
		Dynamic event (frequency jump)	Fail	The GFM inverter does not respond to frequency changes because it operates in isochronous mode instead of droop mode.	
		Dynamic event (phase jump)	Need improvements	The GFM inverter does respond to the phase jump but there is oscillations. This performance needs to be improved by better damping capability.	
		Inertia response test	Fail	The GFM inverter does not respond to frequency changes because it operates in isochronous mode instead of droop mode.	
	Transition operation	Transient	Synchronize a small system to the grid, and islanding	Pass	Has smooth synchronization operation but has very large transients in voltage and frequency during islanding operation.